Detectors for the James Webb Space Telescope near-infrared spectrograph

Bernard J. Rauscher[*a], Donald F. Figer[c], Michael W. Regan[c], Torsten Böker[b], James Garnett[f], Robert J. Hill[e], Georgio Bagnasco[b], Jesus Balleza[c], Richard Barney[a], Louis E. Bergeron[c], Clifford Brambora[a], Joe Connelly[a], Rebecca Derro[a], Mike DiPirro[a], Cristina Doria-Warner[a], Aprille Ericsson[a], Stu Glazer[a], Charles Greene[a], Donald N.B. Hall[d], Shane Jacobson[d], Peter Jakobsen[b], Eric Johnson[a], Scott D. Johnson[a], Carolyn Krebs[a], Danny J. Krebs[a], Scott Lambros[a], Blake Likins[a], Sridhar Manthripragada[a], Robert J. Martineau[a], Ernie Morse[c], S. Harvey Moseley[a], D. Brent Mott[a], Theo Muench[a], Hongwoo Park[a], Susan Parker[d], Elizabeth Polidan[a], Robert Rashford[a], Kamdin Shakoorzadeh[g], Raveev Sharma[a], Paolo Strada[b], Augustyn Waczynski[a], Yiting Wen[a], Selmer Wong[f], John Yagelowich[a] & Monica Zuray[a]

[a]NASA Goddard Space Flight Center, Greenbelt, MD, 20771, U.S.A.
[b]ESA European Space Research & Technology Centre, 2200 AG Noordwijk, Netherlands
[c]Space Telescope Science Institute, 3700 San Martin Drive, Baltimore, MD, 21218, U.S.A.
[d]Institute for Astronomy, 640 N. Aohoku Pl., Honolulu, HI, 96720, U.S.A.
[e]Science Systems & Applications Inc., Greenbelt, MD, U.S.A.
[f]Rockwell Scientific, 5212 Verdugo Way, Camarillo, CA, 93012, U.S.A.
[g]QSS Group, Seabrook, MD, U.S.A.

ABSTRACT

The Near-Infrared Spectrograph (NIRSpec) is the James Webb Space Telescope's primary near-infrared spectrograph. NASA is providing the NIRSpec detector subsystem, which consists of the focal plane array, focal plane electronics, cable harnesses, and software. The focal plane array comprises two closely-butted $\lambda_{co} \sim 5$ μm Rockwell HAWAII-2RG sensor chip assemblies. After briefly describing the NIRSpec instrument, we summarize some of the driving requirements for the detector subsystem, discuss the baseline architecture (and alternatives), and presents some recent detector test results including a description of a newly identified noise component that we have found in some archival JWST test data. We dub this new noise component, which appears to be similar to classical two-state popcorn noise in many aspects, "popcorn mesa noise." We close with the current status of the detector subsystem development effort.

Keywords: JWST, NIRSpec, Infrared, Detectors, HAWAII-2RG

1. INTRODUCTION

The purpose of this paper is to provide a snapshot of the developmental status of the James Webb Space Telescope (JWST) Near-Infrared Spectrograph's (NIRSpec's) detector subsystem (DS). It includes summaries of the requirements, system architecture, and recent detector test results. NIRSpec is JWST's primary near-infrared (NIR; $\lambda = 0.6 - 5$ μm) spectrograph. NIRSpec is being built by European industry, under ESA leadership, and with ESA funding. For readers who may not be familiar with JWST, we begin by providing a high-level overview of NIRSpec. Readers who require more information should see the companion papers in this volume. This is followed by discussions of the requirements, baseline system architecture, test results, popcorn mesa noise, status, and a summary.

2. JWST NEAR-INFRARED SPECTROGRAPH (NIRSPEC)

NIRSpec is a state-of-the-art NIR multi-object spectrograph, designed to be capable of obtaining spectra of 100 or more astronomical sources simultaneously at a spectral resolution of $R \equiv \lambda/\Delta\lambda \sim 100$ over the $\lambda = 0.6–5$ μm wavelength range, or at a spectral resolution of R~1000 over $\lambda = 1–5$ μm. The R~100 mode employs a single prism as its dispersive

---

element and is intended for measuring the redshifts and continua spectra of faint galaxies. The R~1000 mode utilizes three diffraction gratings to cover the $\lambda = 1 - 5$ μm spectra region, and is primarily intended for detailed follow-up observations using conventional nebular emission lines as astrophysical diagnostics. Lastly, three R~3000 gratings also covering $\lambda = 1-5$ μm will allow kinematic studies of individual galaxies to be carried out in single object mode.
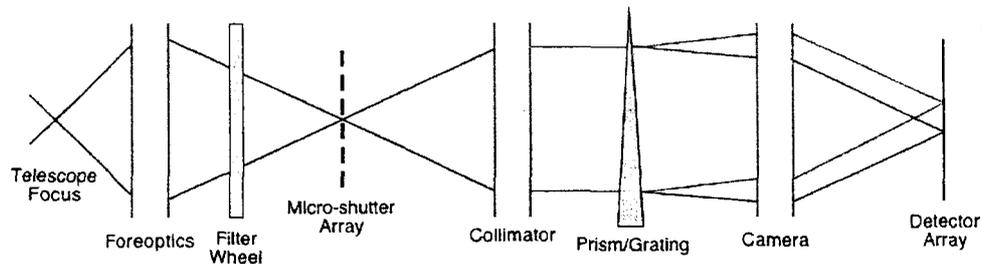

Figure 1. Schematic of the NIRSpec optical system.

The NIRSpec design employs all reflective optics, with most of its optical and structural elements manufactured out of modern ceramic materials (SiC and/or C-SiC). The optical chain (Figure 1) has three main components. The fore-optics re-image and magnify the focal plane image of the JWST telescope onto the slit selection mechanism. The collimator converts the light emerging from each slit into a parallel beam and projects it onto the grating wheel which carries the six (flat) reflective gratings, the (dual pass reflective) prism and a mirror flat for target acquisition. The camera finally focuses the dispersed collimated light coming off the grating onto the detector array. A filter wheel located in an internal pupil of the fore-optics carries the requisite order separation filters for the diffraction gratings and also serves as the instrument shutter.

The NIRSpec slit selection mechanism (Figure 2) is a programmable Micro Shutter Array (MSA) to be provided by NASA. The MSA is made up of four 384 x 175 sub-arrays of individually programmable shutters. The open area of each shutter is 200 milli-arcseconds wide and 450 milli-arcseconds long. The active area of the whole MSA spans a field of view measuring 9 square arc-minutes on the sky. In addition to the programmable micro shutters, the MSA also carries several fixed slits that can be used for high contrast observations of single objects at any of the three spectral resolutions. Resources permitting, a passive small field (~3x3 arcmin^2) Integral Field Unit (IFU) may also be included for use with the three R~3000 gratings.
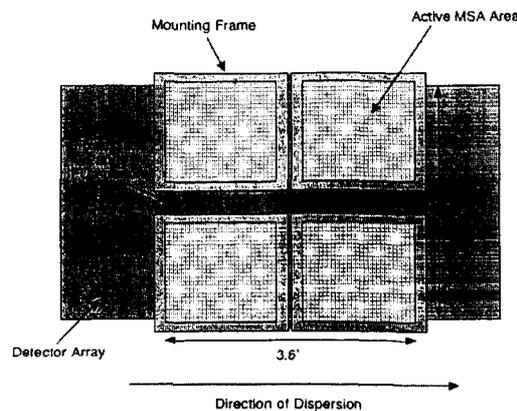

Figure 2. Schematic layout of the NIRSpec slit mask overlaid on the detector array.

The NIRSpec DS consists of two closely butted 2Kx2K pixels^2 Rockwell HgCdTe detector arrays, which will also be provided by NASA and are the subject of this paper. In order to optimize the detector noise limited faint-end sensitivity of NIRSpec, the detector samples the spectra at a relatively coarse 100 milli-arcseconds per pixel.

NIRSpec is expected to be capable of reaching continuum fluxes approaching ~125 nJy at S/N~10 in t~10^4 s in R~100 mode, and line fluxes as faint as ~5 x 10^{-19} erg s^{-1} cm^{-2} at S/N~10 in t~10^5 s in R~1000 mode.

The prime contractor for NIRSpec is presently in the process of being selected and will be announced in late June 2004.

3. DETECTOR SUBSYSTEM PERFORMANCE REQUIREMENTS

The DS requirements include Functional and Performance Requirements, and other requirements of a more implementation dependent and/or programmatic nature. Because we believe that most readers who's background is astronomical telescopes (the title of this conference) will be primarily interested in the Functional and Performance Requirements, we include a brief summary here (Table 1).

TABLE 1. HIGHLIGHTS OF NIRSPEC DS FUNCTIONAL & PERFORMANCE REQUIREMENTS[1,2]

Parameter	Requirement	Comments
Operating wavelength range	0.6 – 5 μm	
Total Noise per pixel	<6 e⁻ rms	To be computed as mean value over all operable pixels in a MULTIACCUM-84 sampled exposure, over 1000 seconds, and using multiple images.
Mean Dark Current per pixel	<0.01 e⁻/s/pixel	
Readout scheme	The total noise requirement will be achieved with a non-destructive readout scheme consistent with the foreseen NIRSpec on-board processing capabilities and telemetry rate; i.e. only straight addition of reads on-board and downlink of one summed Frame every 50 sec.	
Mean DQE over all pixels	$0.6 < \lambda < 1.0$ μm, DQE ≥ 70% $1.0 \le \lambda < 5.0$ μm, DQE ≥ 80%	We specify detective quantum efficiency (DQE) because it correctly allows for the possible creation of multiple electrons per incident photon at short λ. All values include AR coatings, if any.
Maximum gradient in DQE	≤3% / 0.01 μm	Defined as d(DQE)/dλ
DS response linearity	<10%	Defined from 0 – 90% of full well.
Pixel-to-Pixel non-uniformity	<10%	Defined as the standard deviation of response with respect to the mean response of all pixels defined as simultaneously operable for both science and target acquisition.
Frame readout time	12 s	This is the time to clock and digitize 2K×2K pixels.
SCA to SCA gap	≤3 mm	Pixel edge to pixel edge
Cutoff wavelength sensitivity	<1%	Sensitivity <1% for λ > 6 μm
Well capacity	6×10^4 e-	
Pixel crosstalk	<5%	λ = 1 – 5 μm
Fringing	<3%	
Radiometric Instability	short term (1000 s), 0.1% long term (>2 mos.), <5 %	

Parameter	Requirement	Comments
Focal Plane Array (FPA) imaging surface flatness	≤50 μm peak-to-valley	Across full 4K×2K FPA. Includes inherent sensor chip assembly (SCA) flatness and positioning of one SCA relative to the other. At the time of writing, this requirement was being re-negotiated to specify the maximum allowable excursion relative to the best fitting plane across the full FPA rather than "peak-to-valley."
Pixel operability for science	>92%	A pixel is "operable for science" if it does not belong to one of the following 2 classes: (1) dead/low-DQE pixels and (2) noisy pixels. A dead/low-DQE pixel is one that deviates by more than 30% from the mean DQE value. A noisy pixel is a pixel with total noise >12 e- per 1000 seconds multiply-sampled exposure.
Pixel operability for target acquisition	>97%	A pixel is operable for target acquisition if it does not belong to any of the following two categories: (1) dead pixels and (2) noisy pixels. A dead pixel is one with no radiometric response. A noisy pixel is one with total noise >21 e- per Fowler-8 exposure
Latent (or residual) images	<0.1%	First read, after a maximum of 3 resets, immediately following a 12 s exposure with fluence ~full well.

[1]In some cases, we have slightly changed the wording for clarity in the context of this paper. In case of conflicts or inconsistencies, the NIRSpec Functional Performance and Requirements Document (ESA-JWST-RQ-22) takes precedence.

[2]Some of these requirements are marked to-be-reviewed (TBR) in the actual NIRSpec requirements documents. For brevity, and because the TBR items are subject to revision by mutual agreement of ESA and NASA, we have deleted TBR designations here.

4. DETECTOR SUBSYSTEM ARCHITECTURE

The DS architecture consists of the Focal Plane Assembly (FPA), Focal Plane Electronics (FPE), sensor chip electronics (SCE) to SCA harnesses, and Operational Temperature Control harnesses. Figure 3 shows the major components of the baseline DS. Figure 4 shows an exploded assembly drawing of an individual SCA.

A recent technological development that we are closely following is Rockwell's System for Image Digitization, Enhancement, Control and Retrieval (SIDECAR[1]) application specific integrated circuit (ASIC; hereafter referred to as the "ASIC"). Although the baseline concept uses a classical set of readout electronics, we plan to undertake a trade study later this year to determine whether or not to use an alternative architecture designed around the ASIC. These issues will be discussed in more detail below.

The FPA assembly provides the mechanical, electrical, and thermal interface for two 2K×2K pixels[2] HAWAII-2RG (H2RG) SCAs. The SCA modules are fastened to a molybdenum mosaic plate. Molybdenum is chosen for its good thermal contraction match to the SCA modules and for its high thermal conductivity. The mosaic of SCAs is supported

off of a titanium baseplate with titanium standoffs which provide both thermal isolation and mechanical compliance between the different materials of the mosaic plate and titanium baseplate during cryogenic operation. The baseplate is the critical interface to the instrument for thermal, optical, mechanical and electrical interfaces.
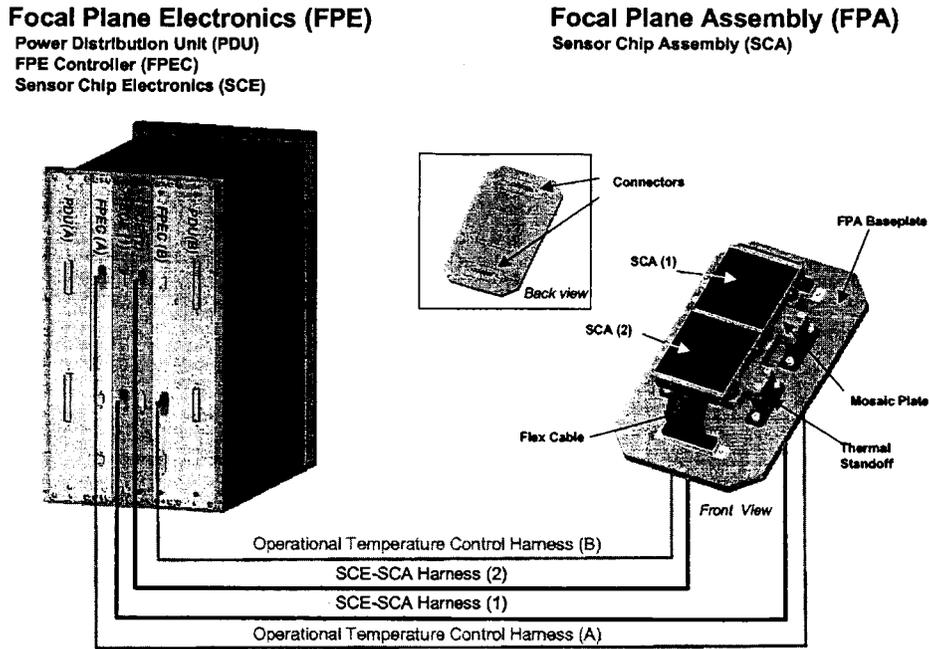

Focal Plane Electronics (FPE)
Power Distribution Unit (PDU)
FPE Controller (FPEC)
Sensor Chip Electronics (SCE)

Focal Plane Assembly (FPA)
Sensor Chip Assembly (SCA)

Figure 3. The baseline DS concept consists of Focal Plane Electronics, cable harnesses, and a 4K×2K pixels^2 HgCdTe focal plane array. These components are described in more detail in the text.

Each SCA is connected to the FPE by an SCE-SCA harness. The SCE-SCA harnesses mate to the flight-qualified micro-D miniature connectors shown in the back view of the FPA (Figure 3). The FPA design is modular in that each SCA is mechanically separate from the other. In the event that an SCA needs to be replaced, the entire FPA assembly would be sent to the vendor where this could be straightforwardly done on account of the modular design. All interfaces are precision machined and pinned allowing for repeatable assembly.

The FPE provides the required biases and clocks to the FPA and samples the sensitive analog output signal from the detector. This includes waveform shaping of clocking signals going to the FPA (including e.g. use of active and passive components to minimize ringing at edges) and analog-to-digital conversion of the output data. The FPE also provides FPA temperature stability to better than $\Delta T = 20$ mK through active control of the FPA heaters and utilizing the FPA sensors, both of which will likely be mounted to the back side of the mosaic plate.

The baseline FPE architecture consist of the following components; power distribution unit (PDU), FPE controller (FPEC) and the SCE. The PDU and FPEC are cold spare redundant, meaning that the spare is only used if the primary unit fails. The PDU uses the 28 Volts DC provided by the spacecraft to supply all the secondary voltages required to run the FPA. The FPEC is responsible for commanding the FPA to start science observations and for receiving science and housekeeping data from the FPA. In addition, temperature control circuitry resides on this card.

The Operation Temperature Control harness carries the temperature control data to and from a heater and sensor on the FPA. The thermal control system is also cold spare redundant as shown by the A and B components in Figure 3. The SCE provides all clocks and biases to properly operate the SCAs. The SCE also amplifies and digitizes the analog output from the SCAs to 16-bit digital data. As shown in Figure 3, SCE (1) connects to SCA (1) via the SCE-SCA harness (1). In the same way SCE (2) connects SCA (2) via SCE-SCA harness (2). The two SCA-SCE systems are independent of each other providing some redundancy.
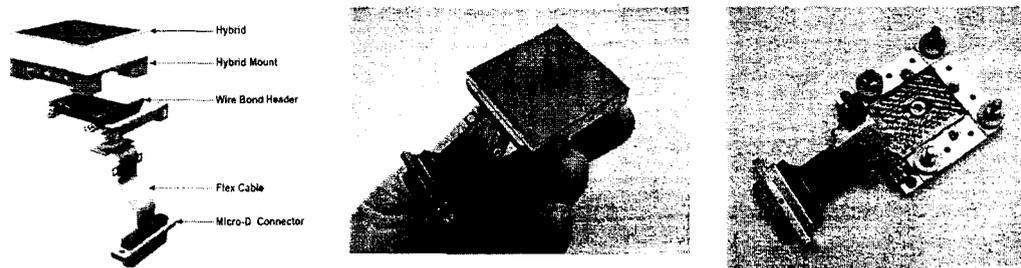
Figure 4. NIRSpec uses two Rockwell H2RG Sensor Chip Assemblies (SCA's) sensitive over the $\lambda = 0.6 - 5 \ \mu$m wavelength range. From left to right are shown: (1) exploded assembly view of SCA, (2) SCA viewed from top, photo-sensitive side, and (3) SCA viewed from underside. The Hybrid consists of a substrate-removed HgCdTe detector array indium bump-bonded to a H2RG readout integrated circuit (ROIC).

The SCE-SCA harness allows for a low noise electrical interface between the FPE and FPA. The proposed SCE-SCA harness is a double shielded flat ribbon cable approximately 4 meters long, 4 cm wide, and 0.5 cm thick. The proposed Operational Temperature Control harness would be a flat ribbon cable of similar design.

In the preceding paragraphs, we have described the baseline architecture which is based on a classical set of focal plane electronics. An alternative concept using Rockwell's SIDECAR ASIC[1] is also being considered. If the ASIC demonstrates that it can meet noise requirements during testing at U. Hawaii during the summer of 2004, the DS Team, in consultation with ESA, will make a decision on whether or not to change the architecture. These changes would be system-wide. If we adopt this approach, a primary motivation will be to improve performance. Amongst other things, this would be accomplished by reducing the risk of electro-magnetic interference by eliminating the 4 meter long harness that carries the sensitive SCA analog output signals to pre-amps in the SCE.

5. DETECTOR TEST RESULTS

NIRSpec's $\lambda_{co} \sim 5 \ \mu$m HgCdTe Rockwell H2RG detectors were extensively tested during JWST's Phase-A detector development program (see [2]). Although the Phase-A detector development program has ended, we continue to analyze the archival data that were collected at U. Hawaii and at the Independent Detector Testing Laboratory (IDTL). The IDTL is located on the campus of Johns Hopkins University and is jointly operated by the Space Telescope Science Institute (STScI) and Johns Hopkins University. Here we present some of these results, with an emphasis on exploring the affects of using more flight-representative calibration and analysis software.

Our ongoing analysis of archival data has revealed a noise component that was not previously recognized during JWST testing. We have dubbed this new component "popcorn mesa noise", due to its similarity to classical two-state popcorn noise (with a relatively long wait in the "high" or "low" states), and have dedicated Section 6 to describing the effect as we understand it today. Since the popcorn mesa noise is somewhat new to the JWST community, our discussion focuses on describing the effect with an aim toward enabling follow-up studies to identify, and if possible fix, the underlying cause.

In the remainder of this section, we provide an update on total noise and dark current testing results using flight representative readout modes and calibration software.

5.1. Flight representative SCA readout and calibration

The principal difference between the current analysis compared to the more general JWST detector testing and calibration that was done during Phase-A is that we are using more flight-representative calibration software.[1] Much of the earlier testing, especially in the IDTL, was done using sampled-up-the-ramp data cubes that were subsequently calibrated as per Fowler sampling. The U. Hawaii data were calibrated in several ways, including slope fitting and Fowler type calibration; although the details of which pixels were included or excluded from a particular test differed somewhat compared to today. Likewise, the earlier U. Hawaii analysis did not mask out popcorn mesa noise since the effect had not yet been recognized. Summarizing the differences; (1) all calibration of long DARK exposures is now being done using slope fitting, (2) the software flags and excludes cosmic ray hits, and (3) the software flags and excludes pixels that are strongly affected by popcorn mesa noise. We believe that this is perhaps the first time that condition 3, excluding popcorn mesa noise, has been rigorously applied to data from a JWST prototype H2RG SCA. In the following paragraphs, we describe Fowler sampling and MULTIACCUM readout, and then summarize some test results.
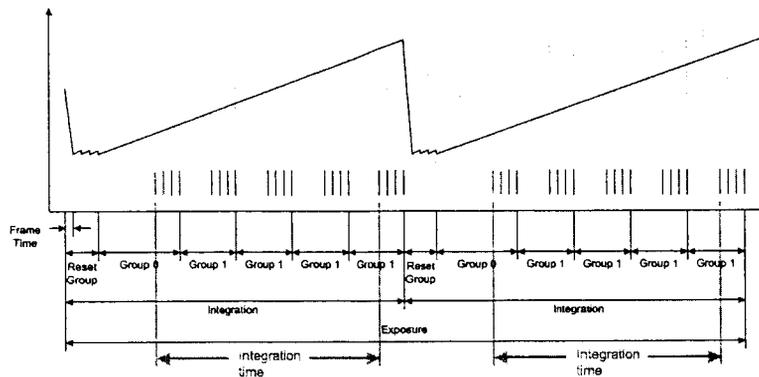

Figure 5. MULTIACCUM sampling. For flight operations, STScI has defined a lexicon of terms that will be used to describe JWST MULTIACCUM sampled observations. Because this usage may differ to that used by other missions or ground-based observatories, we include a short description of the parameters here. At the top level, JWST defines an EXPOSURE. Each EXPOSURE may contain one or more INTEGRATIONS. An INTEGRATION is a unit of data that begins by destructively resetting the detector one or more times and then beginning to take FRAMES of samples at the frame rate. A FRAME is one read of a rectangular area of the detector. On orbit, FRAMES will normally be averaged into GROUPS. For NIRSpec, there will typically be one GROUP generated every 48 seconds.

In Fowler sampling, one clocks and digitizes all pixels in a rectangular area of the SCA at a fixed frame rate. A group of frames is averaged at the beginning of the integration, and a group is averaged at the end. The difference between these two averages gives the integrated signal. One can optionally clock (or not clock) the SCA between taking groups of frames. As an example of Fowler sampling, consider a 1000 seconds JWST Fowler-8 integration. The integration timer starts when the 0th pixel of the zeroth frame is sampled and stops when the 0th pixel of the 8th frame is sampled, where frame number $\in \{0\text{-}15\}$. One begins the integration by resetting all pixels and then non-destructively sample each pixel 8× near the beginning of the integration at a 12 seconds/frame rate, wait 1000 seconds after digitizing the zeroth pixel of the zeroth frame, and then non-destructively sample the pixel 8× again at the end at the nominal 12 seconds/frame rate. One generally clocks and digitizes all pixels in the rectangular region before digitizing any given pixel again.

While Fowler sampling is very good at averaging down many noise components, it is not the baseline for NIRSpec science observations. This arises because NIRSpec must operate in the cosmic ray environment at L2. During a planned 1000 seconds integration, as many as 10-20% of the pixels will typically be hit by cosmic rays. In Fowler sampling as it is usually implemented, these pixel data are lost. A powerful alternative is to use a generalized type of sampling-up-the-ramp that has been dubbed MULTIACCUM by the JWST Project. Because cosmic ray hits can be recognized as

---

[1]Additional comprehensive testing is planned for NIRSpec once Rockwell begins to produce SCAs under contract. Until these new SCAs start to become available, NIRSpec laboratory testing is focused on radiation testing.

transients in the pixel ramps as signal accumulates at a steady rate, powerful ground-based software can identify hits and, it is hoped, continue the integration in a given pixel even though it has been hit by a cosmic ray. Although a few samples may be lost close to the time of the hit, our aim is to use the data from most of the samples-up-the-ramp. If this approach works (further study using ground test data that have been corrupted by cosmic rays and/or protons is planned), we eventually plan to take integrations significantly longer than 1000 seconds. For NIRSpec, this would pay significant sensitivity dividends since there would be less read noise (on account of the smaller number of destructive resets) in a typical science data set (see [3] for a discussion of the benefits of longer integrations).
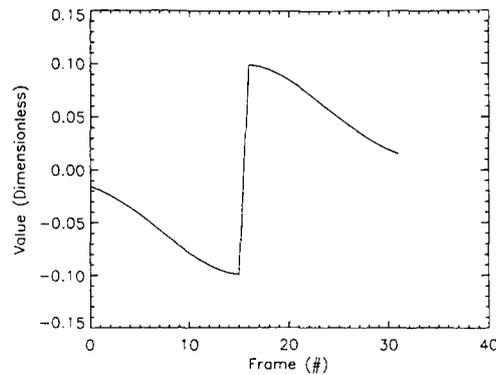

Figure 6. Kernel for finding cosmic ray hits and popcorn mesa noise. When this kernel is convolved with the integrating signal in a pixel ramp, normal cosmic ray hits (step-up) generate a strong peak. Popcorn mesa noise on the other hand generates strong positive and negative spikes of roughly comparable amplitude. The precise number of frames used in the kernel (here 32) is determined by the number of samples up-the-ramp. In practice, we have found that the kernel shown here is good when there are about 250 up-the-ramp samples. When fewer samples are available going up-the-ramp, a narrower kernel is used.

In the JWST MULTIACCUM readout mode, pixels are sampled non-destructively up-the-ramp. Figure 5 shows an example of how MULTIACCUM works in practice. An important difference compared to some earlier testing is that up to 84 non-destructive samples may be used to construct a 1000 seconds NIRSpec integration, as opposed to 16 samples in the earlier Fowler-8 readout. The use of more samples facilitates lower total-noise operation. It also facilitates cosmic ray and popcorn mesa noise identification.

We find both cosmic ray hits and popcorn mesa noise by convolving the integrating signal in each pixel's ramp with the kernel shown in Figure 6. Typical cosmic ray hits look like a positive step up in the ramp. These result in a strong positive peak when the ramp is convolved with the kernel. Popcorn mesa noise, on the other hand, results in several strong positive and negative going peaks. For both cosmic ray hits and popcorn mesa noise, we typically use a 5σ criterion for determining whether a peak in the convolved ramp is significant or not. For those pixels that are flagged, the software notes whether it is a normal cosmic ray hit or popcorn mesa noise. In the case of normal cosmic ray hits, the affected pixel is flagged as a hit and nearby neighbors are flagged as cosmic ray neighbors. In the case of popcorn mesa noise, the software marks only the affected pixel. The kernel is not good at finding transients that persist for significantly fewer frames than the kernel width. While this is not a problem for normal cosmic rays, which step up and do not decay back down, it does cause us to underestimate the amount of popcorn mesa noise, particularly when the amount of time spent in the "high" or "low" state is very short.

5.2. Total noise using flight-representative readout and calibration

During JWST's phase-A phase-A detector development program, at least two $\lambda_{co} \sim 5$ μm Rockwell H2RG SCAs were produced that were consistent with NIRSpec's system-level 6 e- rms total noise requirement during testing at U. Hawaii. More specifically, the requirement is for the DS to contribute no more than 6 e- rms on average per 1000 seconds exposure and using up to 84 multiple non-destructive samples up the ramp. In the analysis of SCA H2RG-015-5.0mu, the NIRSpec Team has processed 84 frame sampled-up-the-ramp exposures into flight-like MULTIACCUM-21×4 data

cubes and calibrating them using a prototype version of the calibration pipeline that will be used for acceptance testing and characterization. The notation MULTIACCUM-21×4 indicates that the SCA is clocked continuously and that groups of 4 frames are averaged together yielding 21 groups sampling-up-the-ramp at 48 seconds intervals. Due to data volume limitations in the U. Hawaii test setup at the time the data were taken, the SCA H2RG-006-5.0mu have been calibrated in a manner that is intended to mimic the acceptance testing, although not be identical to it.

In the remainder of this section, we focus on the two SCAs mentioned above. SCA H2RG-015-5.0mu met the total nosie requirement using flight-representative readout modes and calibration. Although we believe that SCA H2RG-006-5.0mu would meet requirements when operated and calibrated in this manner, analysis is ongoing to show that this is actually the case. Here we present some available data showing that the SCA was consistent with requirements using a readout mode intended to mimic MULTIACCUM-21×4. Within a few weeks, we plan to complete analysis of additional data to confirm that the SCA meets requirements when operated and calibrated in the planned manner.

5.3. SCA H2RG-015-5.0mu

Substrate-removed SCA H2RG-015-5.0mu was Rockwell's "homerun" device during Phase-A and was the detector that was submitted for comparative testing in the detector competition that was ongoing at the time. During testing at U. Hawaii, this SCA met NIRSpec's system level 6 electrons rms total noise per ~1000 seconds exposure requirement. Figure 7 and Figure 8 provide additional information on these test results.
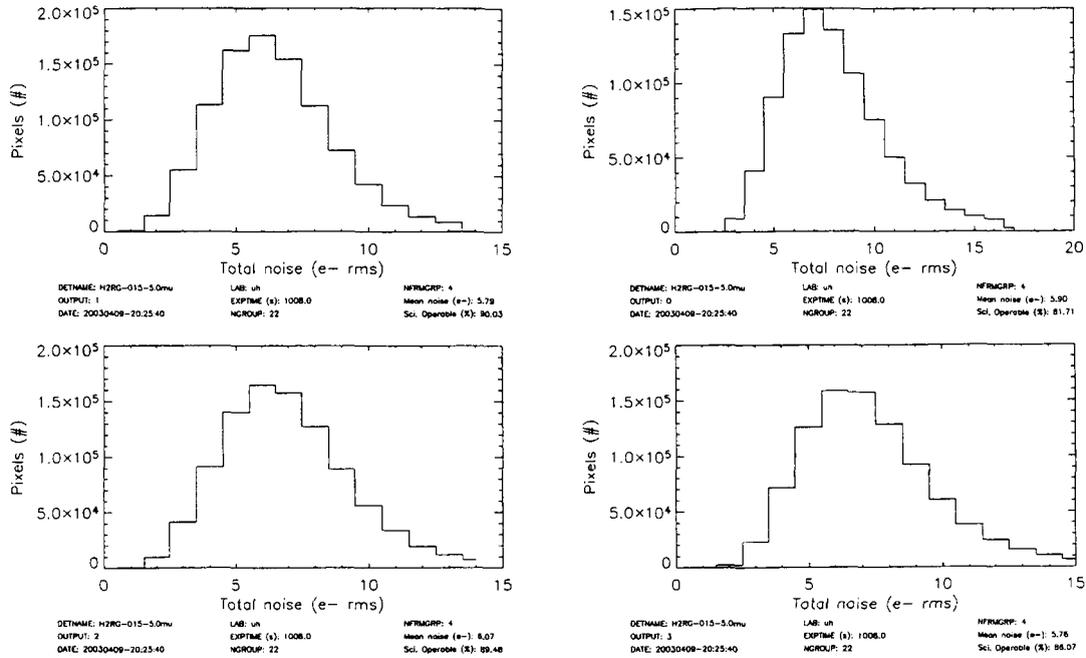
Figure 7. Noise histograms per 1 Megapixel output of SCA H2RG-015-5.0mu (see Figure 8 for an aggregate histogram). This test met the NIRSpec system-level total noise requirement using flight-representative readout and calibration. These data were taken at U. Hawaii using the NIRSpec baseline MULTIACCUM sampling method. The data consisted of 5 identical t=1008 seconds DARK exposures. At the start of each DARK, the each pixel in the SCA was reset twice using a pixel-by-pixel reset scheme at the normal readout rate. The SCA was stabilized to a temperature T=37.000 ± .001 K for the duration of the experiment. The Frame rate was 12 seconds/frame, and groups of 4 frames were averaged to yield one average group every 48 seconds going up the 1008 seconds ramp. Although the system met the NIRSpec total noise requirement, the SCA does not quite meet the 92% Operability for Science requirement. For the actual NIRSpec DS acceptance testing, a to-be-determined (TBD) statistical correction will be made to the raw operability numbers to account for the uncertainty in measuring the noise of a pixel when using modest (≤25) numbers of exposures and the bias that this introduces on the positive side of the histogram peak. This statistical correction will be mutually agreed to by ESA and NASA.
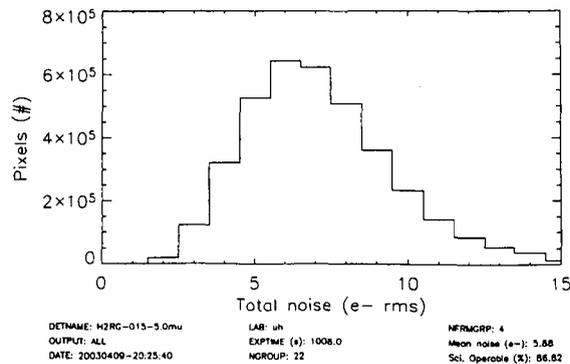

Figure 8. Noise histogram for all outputs of SCA H2RG-015-5.0mu. As per Figure 7, a TBD statistical correction must be made to the "Sci. Operable" number to account for bias introduced by uncertainties in measuring the noise of any one pixel using small (≤25) number of exposures.

5.3.1. SCA H2RG-006-5.0mu

SCA H2RG-006-5.0mu was a very high quality substrate-removed SCA that was produced early in the program. While testing it, U. Hawaii conducted a limited number of tests using readout modes that were matched, to the extent possible within data volume limitations at the time, to NIRSpec requirements for measuring total noise per pixel. These tests used 32 identical sampled-up-the-ramp DARK exposures, each of 145 frames, for a total integration time of 58,000 seconds. Each exposure was preceded by two pixel-by-pixel resets of the SCA at the normal pixel readout rate.

Due to data storage limitations, the first nine frames and the final eight frames of sampled-up-the-ramp exposures were written to disk. Slope images (calibrated as per Fowler-sampling, although the data were sampled-up-the-ramp) were formed by subtracting averages of initial frames from averages of final frames to generate 32 ramps x 2048 x 2048 pixels cubes processed as per Fowler-2^n, for $n \in \{0, 1, 2, 3\}$. The highest pixel value among the 32 in each pixel string was discarded to account for cosmic ray effects. The mean of each pixel string estimates the dark current and the standard deviation of each pixel string estimates the total noise in an exposure. During calibration, pixels having dark current $i_{dark} > 0.025$ e-/sec were flagged as inoperable and excluded. Adjacent ramps were averaged to simulate Fowler-16 and Fowler-32 total noise from the existing data. Figure 9 shows the total noise per output of SCA H2RG-006-5.0mu as tested and calibrated by the U. Hawaii.

This procedure is not identical to what will be done during NIRSpec acceptance testing and calibration, and care should therefore be used in interpreting the results. Nevertheless, it does provide an indication that Rockwell H2RG SCAs are capable of meeting even the challenging 6 e- rms total noise requirement.
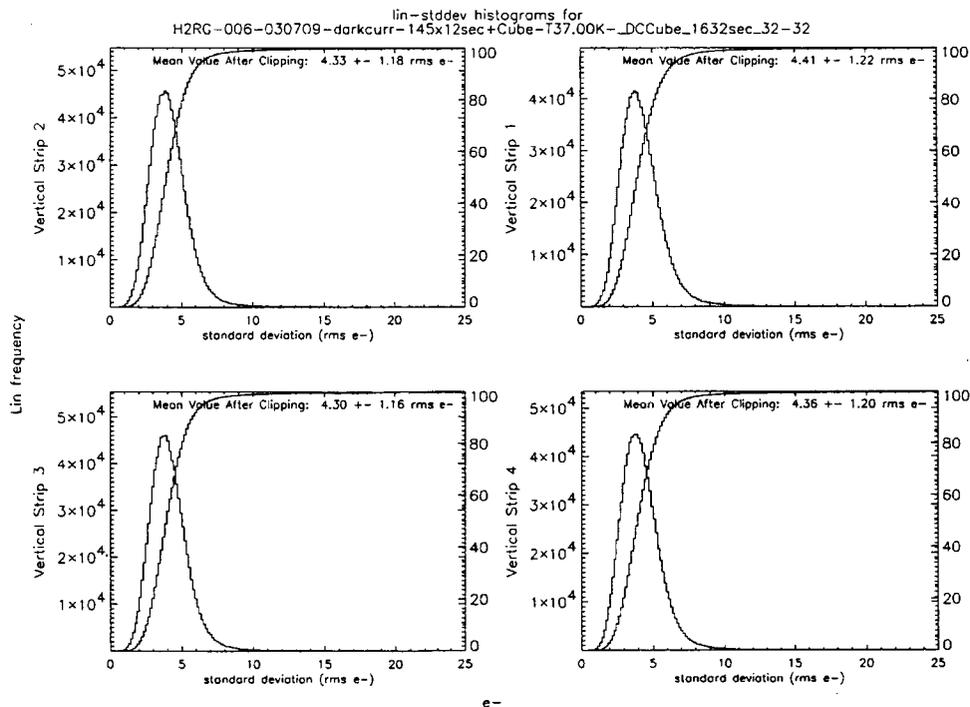

Figure 9. Substrate-removed SCA H2RG-006-5.0mu demonstrated outstandingly low total noise during testing at U. Hawaii. Plots are of each of the 1 Megapixel outputs of the SCA and represent the total noise in an 1632 second exposure. The technique for obtaining and analyzing these data is described in Section 5.3.1. The data were sampled-up-the-ramp and post-processing was used to construct exposures that U. Hawaii believes are indicative of "Fowler-32" sampling. Fowler sampling differs from the NIRSpec MULTIACCUM baseline which allows up to 84 non-destructive samples-up-the-ramp. Because of data volume limitations in the U. Hawaii test setup at the time, the calibration procedure was fairly detailed and the interested reader should be careful to understand the description given in Section 5.3.1 of the text.

5.4. Dark current

At least two SCAs, H2RG-006-5.0mu and H2RG-015-5.0mu met NIRSpec's 0.01 e-/s/pixel dark current requirement. Figure 10 shows the measured performance during testing at U. Hawaii and in the IDTL. In the IDTL data, dark current was measured relatively soon after making temperature changes. In these data, the first measurement is occasionally anomalous. We speculate that this may indicate some annealing, bias instability, or hysteresis in how the reference pixels track the normal light sensitive pixels.
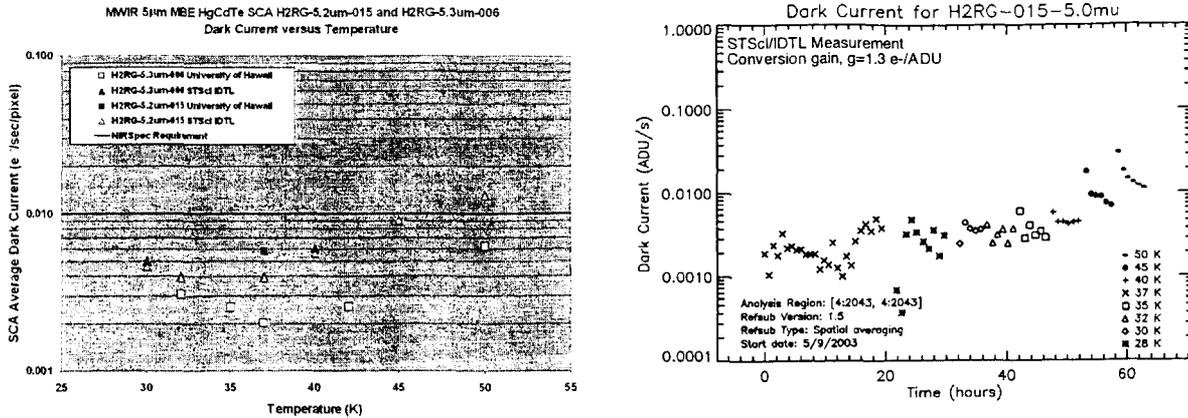

Figure 10. The $\lambda_{co} \sim 5$ μm Rockwell H2RG detectors that will be used by NIRSpec demonstrated dark current consistent with the instrument's challenging dark current requirements during Phase-A testing at U. Hawaii and in the IDTL. At left, average dark current over all light-sensitive pixels is plotted as a function of temperature for two candidate SCAs, H2RG-006-5.0mu and H2RG-015-5.0mu. At right, average dark current over all light-sensitive pixels is plotted as a function of temperature and time at temperature. Both plots show that dark current does not rise steeply with temperature for temperatures T ≤ 40 K. The right hand panel shows some evidence of bias instability and/or annealing shortly after temperature changes. This argues that during normal operations the SCA should be stabilized to one temperature and then held at that temperature for the duration of the scientific program.

5.5. Ultra-low noise radiation testing

Very recently, the team began doing some new radiation testing aimed at exploring how pixel operability is affected by on-orbit radiation effects at the very sensitive ultra-low background levels relevant to NIRSpec. This new phase of radiation testing will explore how pixel operability is influenced and changed at total noise levels, $\sigma_{total} \approx 6$ e$^-$ rms per 1000 seconds exposure, where total noise includes read noise and other noise sources such as shot noise on integrated dark current and $1/f$. Keys to achieving such ultra-low noise performance are i. using flight-like software to process data in the presence of cosmic rays and residual radioactivity in the test setup following irradiation and ii. use of flight-like operating modes which allow up to 84 non-destructive samples-up-the-ramp during a 1000 seconds exposure. The aim of this testing is not to explore noise performance in the beam. Rather, it is to understand how pixel Operability for Science degrades as a function of dose parameters. We anticipate that all ultra-low noise measurements will be done in an infrared test laboratory environment, and only after sufficient time has been allowed for any residual radioactivity in the test setup to decay to flight-representative level of ~5-10 ions cm^{-2} s^{-1}. Changes in pixel operability will be measured by making direct before and after comparisons using the same teams, test setups, and calibration and analysis software.

The ultra-low noise radiation testing will be led by the NASA Goddard Space Flight Center (GSFC) Radiation Effects and Analysis Group (REAG). REAG has selected the Detector Characterization Laboratory (DCL) at GSFC and Craig McCreight's team at NASA Ames Research Center to provide test laboratory support. The NIRSpec Science Team will provide flight-representative calibration and analysis software. The NIRSpec DS Team will provide SCAs for testing.

6. POPCORN MESA NOISE

Some of the $\lambda_{co} \sim 5$ μm HgCdTe Rockwell H2RG SCAs developed for JWST during the Phase-A detector development program show a noise component that we had not previously seen in Rockwell NIR detectors. We have tentatively identified the new noise component as a type of two-state popcorn noise which we refer to as "popcorn mesa noise" (Figure 11). Our rationale for coining the new name was to avoid misleading readers by suggesting that we had identified the physical cause. Moreover, there was a general consensus within the team that adding the descriptive term "mesa" more accurately captured the observed behavior that affected pixels may spend a relatively long time in the "high" or "low" state. We have not yet identified a specific causative mechanism for the popcorn mesa noise. However, we felt that it was important to publish now to enable wider discussion and analysis of the phenomenon.

We have seen popcorn mesa noise in Rockwell H2RG test data from the University of Hawaii and the IDTL, in more than one SCA, in both reference pixels and regular light sensitive pixels (see Figure 12), and in a bare ROIC. Table 2 summarizes the JWST datasets in which we have detected significant amounts of popcorn mesa noise. To rule out the possibility that the popcorn mesa noise was an artifact of the setup, the same software was used to scan IDTL data from a different vendor's NIR SCA in the same test setup and no popcorn mesa noise was found.

TABLE 2. JWST SCAs WITH POPCORN MESA NOISE

TEST LAB	DETECTOR
IDTL	H2RG-015-5.0mu
	H2RG-006-5.0mu
University of Hawaii	H2RG-015-5.0mu
	H2RG-002-0.0mu (a bare ROIC)

Because popcorn mesa is seen in reference pixels (which are not connected to the detector), and in a bare H2RG ROIC, the most likely source appears to be in the ROIC, rather than the HgCdTe detector material or interconnects, although we cannot rule out the possibility that a very small amount of the popcorn mesa noise may originate in the HgCdTe detectors or interconnects. The NIRSpec DS team is working with Rockwell, and others in the JWST Project, to try to pinpoint the source.

In the remainder of this section, we describe what is known about the popcorn mesa noise today, and offer an assessment of the probable science impact for NIRSpec if the popcorn mesa noise cannot be corrected prior to building the flight SCAs. We note that even with the popcorn mesa noise in, SCAs H2RG-015-5.0mu and H2RG-006-5.0mu demonstrated superlative ultra-low background performance consistent with NIRSpec requirements. The data shown in Figure 9 include popcorn mesa noise and meet NIRSpec total noise requirements.

6.1. Description of popcorn mesa noise

The popcorn mesa noise was first noticed while scanning long, 2677 seconds, sampled-up-the-ramp DARK exposures taken in the IDTL for cosmic ray hits. In addition to finding transients, the software attempts to categorize them and record some additional diagnostic information, e.g. the time of the transient, size of the hit, etc. When the software cannot categorize an event, it categorizes it as "other". The popcorn mesa noise was obvious when we started examining these "other" transients.
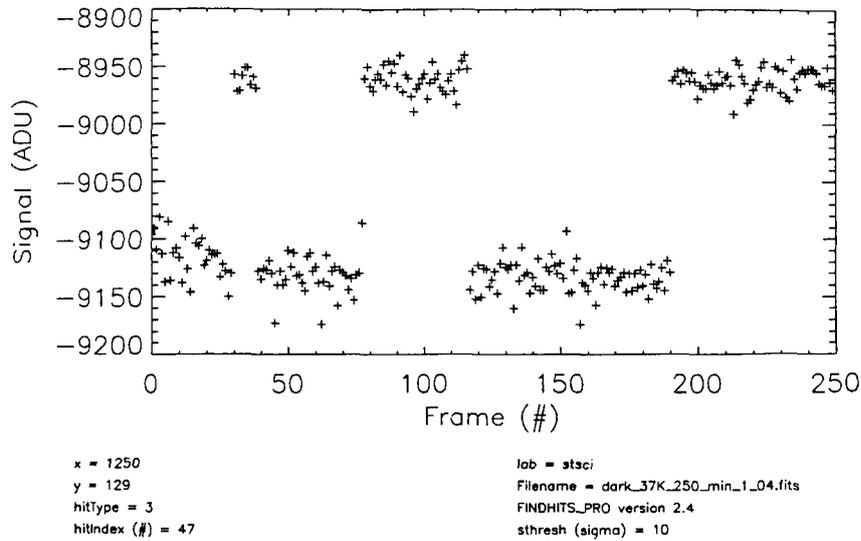
Figure 11. Popcorn mesa noise appears as an almost digital toggling between two states. Here we see the integrating signal in a 2677 seconds DARK exposure of pixel (x,y) = [1250,129] of SCA H2RG-015-5.0mu. The operating temperature was T=37 K, and the conversion gain for this plot is g=1.3 e⁻/ADU. Because these raw data have not been reference pixel corrected, there is a slight negative trend in the slope. When reference pixel correction is performed, this SCA demonstrated excellent dark current of ~0.005 e⁻/s/pixel. Each plus sign represents one ADC sample integrating up-the-ramp at a continuous frame rate =10.7 seconds/frame (we clock through all 2048^2-1 pixels before returning to pixel [1250,129] every 10.7 seconds).

Figure 11 shows a pixel that is affected by popcorn mesa noise. Because these raw data have not been reference pixel corrected, there is a slight downward trend. The popcorn mesa noise manifests itself as an almost binary toggling between states.

In NIRSpec's T=34-37 K detector operating temperature range, we typically detect a few thousand pixels with popcorn mesa noise that is significant at the 10σ level in a 2677 seconds DARK exposure. The affected pixels change from exposure to exposure in an apparently random manner. As such, the popcorn mesa noise is not a property of a few fixed pixels. Rather, in every exposure we find that a small proportion of the pixels (different pixels in each exposure) are affected.

Popcorn mesa noise is seen in both reference pixels and regular light sensitive pixels. Figure 12 shows the probability distributions for both regular and reference pixels in one SCA. Although this limited data set cannot not determine the relative susceptibility of these two classes of pixels, it does demonstrate that both reference pixels and regular pixels are roughly comparably affected. This, together with the observation that popcorn mesa noise was seen in a bare ROIC, argues that most (perhaps all) of the popcorn that we are seeing originates in the ROIC.
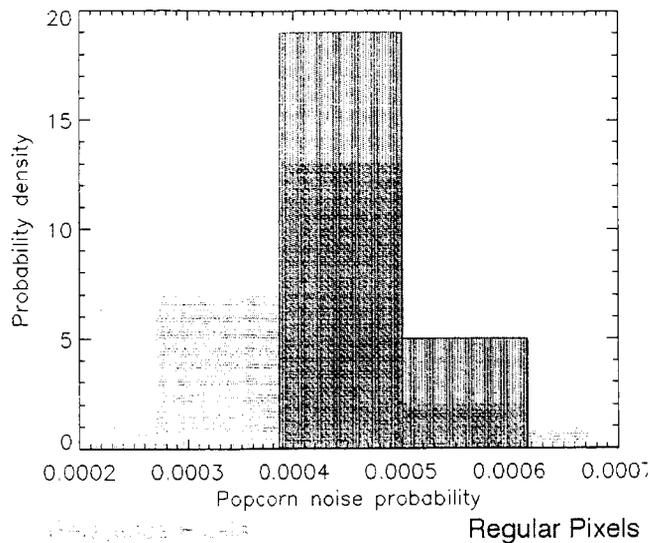
Figure 12. Popcorn mesa noise is seen in regular light sensitive pixels and in reference pixels. There is some preliminary indications that regular pixels might be slighly more prone to popcorn mesa noise.

Preliminary indications are that the number of pixels affected per exposure may be temperature dependent. Specifically, we appear to detect less popcorn mesa noise at higher SCA temperatures. Figure 13 shows the number of pixels of SCA H2RG-015-5.0mu that were affected per 2677 seconds DARK exposure during testing in the IDTL. Unfortunately, both time and temperature are correlated in these data, which were taken before we were aware of the popcorn mesa noise. Nonetheless, there is a long pause between the first group of exposures at T=32 K, and the next group at T=35 K, that helps to break the degeneracy suggesting that temperature is the more important parameter.

The preceding paragraphs summarize our observations of the popcorn mesa noise so far. Additional study is planned, both analyzing data from the existing SCAs, and with additional data from new SCAs that will be produced for NIRSpec. There are still a number of unresolved issues, and some of these are described in the next section.
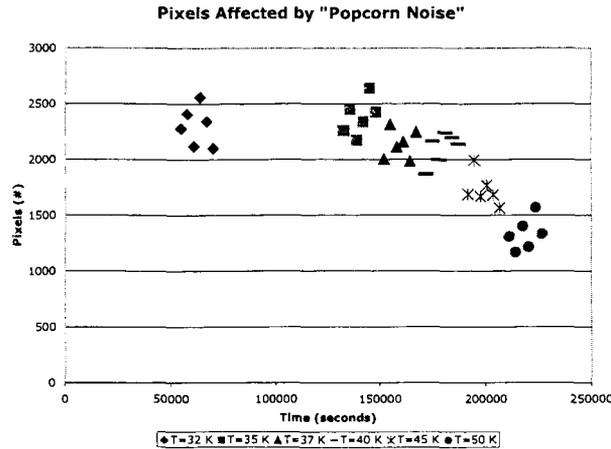
Pixels Affected by "Popcorn Noise"

Figure 13. The number of pixels affected by popcorn mesa noise appears to be temperature dependent, with less popcorn mesa noise at higher temperatures. Here we show the number of pixels having 10σ popcorn mesa noise per 2677 seconds DARK exposure. Although time and temperature are unfortunately correlated in these data, the long pause between $t{\sim}6{\times}104$ and $t{\sim}1.3{\times}10^5$ seconds helps to break the degeneracy suggesting that temperature is the more important parameter.

6.2. Unresolved issues and ongoing studies

There are also indications that the amount of popcorn mesa noise may be influenced by the test setup and/or procedures. For example, the software detects fewer affected pixels in 1728 seconds U. Hawaii darks than in the 2677 seconds IDTL DARKs, even when the data are corrected for the differing exposure time. We are following up this lead by trying to identify which differences between the U. Hawaii and IDTL test setups and procedures are statistically important.

Significant differences between the U. Hawaii test setup, and the IDTL setup that was used during the earlier testing, included the following. (1) U. Hawaii used a more iso-thermal SCA mount that may have reduced internal stress in the SCA[2]. (2) U. Hawaii typically held the SCA at one temperature throughout testing whereas the IDTL explored SCA parameters over a range of temperatures. (3) The two labs used different pixel reset schemes. (4) The IDTL data have more cosmic ray hits. (5) The IDTL testing included many more saturated (or nearly saturated) exposures to explore persistence phenomena. Analysis is ongoing to try to determine if any of these differences is statistically important or not.

In parallel, we have been discussing the popcorn mesa noise with solid state physics experts and the H2RG ROIC designer to try to identify areas in the ROIC where single-charge phenomena could result in signals that are several hundred electrons in size at the SCA output.

6.3. Science impact of popcorn mesa noise

If the popcorn mesa noise in the flight SCAs is no worse than that reported here for the prototype devices operated at T=37 K, the overall impact on the NIRSpec science program will probably be negligible. The primary affect will be to complicate ground-based calibration and analysis software. Specifically, the ground-based software will have to be sophisticated enough to correctly identify and track affected pixels at an approximate $f_{pmn} < 0.1$ pixels cm^{-2} s^{-1} popcorn mesa noise introduction rate. Because f_{pmn} is very small compared to the expected total cosmic ray hit rate under quiescent conditions, $f_{CR} = 5-10$ ions cm^{-2} s^{-1}, we anticipate that tracking the popcorn mesa noise during

---

[2] The IDTL has subsequently re-engineered their SCA mount to conform to iso-thermal design recommendations supplied by Rockwell.

calibration can be straight forwardly handled as part of a larger task of tracking cosmic ray hits and other transient phenomena.

7. STATUS

The status of the NIRSpec DS development effort is as follows. The high level Functional and Performance Requirements have been agreed with ESA and we are in the process of finalizing the Interface Requirements Document with ESA. Designs for a classical set of readout electronics are underway, and we are in consultation with potential vendors for the harnesses. With regard to the FPA, we are in the process of bringing Rockwell under contract. In the area of testing, the Science Team is continuing to analyze archival data from JWST's phase-A detector development program. Some additional data are being taken in concert with NIRCam. These data are primarily focused on assessing the level of thermal stability that is required to meet total noise and other requirements. Study of the popcorn mesa noise is ongoing, with an emphasis on more quantitative statistical studies.

8. SUMMARY

We have described the current developmental status of the JWST NIRSpec DS. This included summaries of the requirements, the baseline architecture, recent test results, and a status update. Analysis of archival data from U. Hawaii shows that two existing H2RG SCAs meet challenging system level NIRSpec total noise requirements using more flight representative readout modes than were used during earlier testing. These are SCAs H2RG-006-5.0mu, having σ_{total} = 4.35 e- rms per t~1000 seconds Fowler-32 sampled exposure, and SCA H2RG-015-5.0mu, having σ_{total} = 5.88 e- rms per t~1000 seconds MULTIACCUM-21×4 sampled exposure. Both of these noise measurements were made using electronic bandwidth =160 kHz measured at the –3 dB frequency and analog gain =40×. About >86.8% of pixels in SCA H2RG-015-5.0mu meet stringent Operability for Science requirements (see Figure 8 & Table 1). Additional analysis is required to determine the percentage of SCA H2RG-006-5.0mu's pixels meet the same Operability for Science requirements. Moreover, analysis of archival JWST data has revealed a new noise component which we call popcorn mesa noise. The popcorn mesa noise appears as an almost digital toggling in the signal in the integrating ramps between "high" and "low" states (see Figure 11). In the data that we have examined so far, the popcorn mesa noise is a small component of the overall noise. Although the baseline architecture uses a classical FPE, harness, and FPA, we are also considering alternatives based on Rockwell's SIDECAR ASIC.

REFERENCES

1. M. Loose, L. Lewyn, H. Darmus, J. Garnett, D.N. Hall, A.B. Joshi, L.J. Kozlowski, & I. Ovsiannikov, 2003, SIDECAR low-power control ASIC for focal plane arrays including A/D conversion and bias generation, Proc. of SPIE Vol. 4841, 782
2. D.F. Figer et al., *Independent detector testing laboratory and the NGST detector characterization project*, Proc. of SPIE Vol. 4850, 140
3. M.W. Regan & H.S. Stockman, 2001, *Optimum integration times for different read modes*, JWST/STScI Technical Memorandum TM-2001-0005 A, http://www.stsci.edu/jwst/docs/tm/TM-2001-0005-A_TM-2001-0005A.pdf